Nanomed Res J 2(4):267-272, Autumn 2017

RESEARCH ARTICLE

Synthesis of Porous Nanostructure NiTi Implant and Measurement of Thermomechanical Properties

Mohammad Saleh Khalatbari[1]*; Maryam Daneshpour[2]

[1]Department of Material Science and Engineering, Sharif University of Technology, Tehran, Iran

[2]Department of Medical Biotechnology, School of Advanced Technologies in Medicine, Shahid Beheshti University of Medical Sciences, Tehran, Iran

ARTICLE INFO

Article History:
Received 21 November 2017
Accepted 19 March 2018
Published 27 March 2018

Keywords:
Nitinol
Superelasticity
Nanostructure
Porosity

ABSTRACT

Objective(s): NiTi is known as the most important material for manufacturing implants and medical devises duo to its shape memory and superelasticity properties, high energy damping, and high corrosion resistance.

Methods: In this project, the possibility of producing nanostructured NiTi implant with high porosity was investigated. For reaching to the nanoscale, the mechanical alloying process was done on Ti and Ni powder as raw materials. Mechanical alloying process and the possibility of reaching nanostructure or amorphous phase was investigated. Space holder technique was used for reaching a porous structure. Sintering process was planned in a way to inhibit grain growth as much as possible. The samples sintered at two different sintering times. The effect of grain size and secondary phases on mechanical properties and phase transformation temperatures was studied.

Results: The results showed that milling for 50 h at 300 rpm has led to amorphous phase and nanocrystallite with 50 nm diameter. Using space holder technique with the appropriate amount of spacer and choosing proper sintering time and temperature, the specimens with 70% porosity were produced. Furthermore, nanoscale grain size can lead to R phase transition. In fact, one of the effects of reaching to nanostructure is occurring R transformation due to high dislocation density and high grain boundaries surface. Nanostructured sample with 70% porosity was shown 5% superelasticity in the cyclic pressure test.

Conclusions: As the results showed, one of the advantages of porous samples is their elastic modulus which is more similar to the bone than other metallic implants.

How to cite this article
Khalatbari M S, Daneshpour M, Synthesis of Porous Nanostructure NiTi Implant and Measurement of Thermomechanical Properties, Nanomed Res J, 2017; 2(4):267-272. DOI: 10.22034/nmrj.2017.04.008

INTRODUCTION

NiTi shape memory alloy (SMA) has frequently been studied over the last three decades. Due to its unique properties, NiTi has been considered as an essential material in different fields of applications such as aerospace [1], surgical instrument [2], endodontic teeth for preparation of the root canals [3], actuators and mechanical dampers [4], oil industries [5], and etc. NiTi displays a wide range of attractive combination of mechanical properties (e.g., good corrosion resistance, appropriate fatigue life, etc.) and functional properties (e.g., shape memory features, large cyclic mechanical energy absorption, and large reversible deformation up to 10% (superelasticity)) [6].

As one of interesting application, there are

* Corresponding Author Email: m.s.khalatbari@gmail.com

numerous studies that have reported the use of porous NiTi as the bone replacement. It is believed that the presence of open pores in this alloy allows tissue propagation while defect remodeling which creates firm in-tissue fixation [7]. Ceramics and metals which are generally used as implant have Young modulus of 100-400 Gpa and cannot match to the bone which has the Young modules of 20Gpa. However, the researchers indicated that porous structure could solve this problem by presenting the porosity that efficiently reduces Young Modules. It has been shown that NiTi with 50% porosity has the Young modules of 14-20 Gpa and 3.2% recoverable strain [8]. The presence of porosity predictably results in decreasing the mechanical strength of this material. However, the mechanical properties can be tailored by designing the pore size, shape, and distribution [9].

Another approach for improving the mechanical properties is reaching to the nanoscale. From the material science point of view, mechanical properties, especially shape memory and superelasticity of NiTi have a close relationship with the microstructure of NiTi. As the studies indicated, lowering the grain size (GS) to nanoscale can lead to broadening super elasticity window and improving cyclic and dynamic stability [10].

Different procedures have been used for the production of porous Nitinol. The major processes are based on powder metallurgy that include conventional element powder sintering [11], hot isostatic pressing (HIP) [12], metal injection modeling (MIM) [13], spark plasma sintering (SPS) [14], self-propagating high temperature synthesis (SHS) [15], and capsule free hot isostatic pressing(CF-HIP) [12]. The pore size, its characteristics, and its distribution obviously vary based on the method used for Nitinol synthesis. As the pore characteristics play the critical role in mechanical properties of fabricated Nitinol, in present study space holder technique has been used to improve pore geometry. Preferable pore dimensions for ordinary orthopedic applications range from 200 μm to 500 μm and the pore controlling spacer should not affect Nitinol. Spacers such as NaCl, NaF, urea, and NH_4HCO_3 have been used in reported studies due to water solubility, heat decomposability, and easy-removing from the system [7].

In this study, conventional sintering via space holder has been used to fabricate NiTi. In order to produce nanopowder, milling raw materials have been used that has been frequently reported in the literature [16, 17]. In addition, the thermomechanical properties of synthesized NiTi such as transition temperature and compression strength are measured.

MATERIALS AND METHODS

Material

Elemental metallic powders of Ti (99.99% Alfa Aesar) and Ni (99.8% GER nickel Merk) were used as raw materials. NaCl was purchased from Sigma.

Experiment

The elemental powders with Ni/Ti atomic ratio of 49.2/50.8 were mechanically alloyed in a planetary ball mill under the argon atmosphere. The high purity argon atmosphere was used to prevent Ti oxidation and TiN formation. The experiment was carried out at room temperature using steel balls. The ball to powder weight ratio and the rotational speed were 10:1 and 300 rpm, respectively. After selected intervals of time and 50h of milling, samples were collected and subjected to X-ray diffraction investigation (XRD, Uniasantic XMD300, GmbH) with Cu-kα radiation (wavelength 1.542 Å) and diffraction angle between 20° and 100°.

In this study, NaCl was used as a spacer which was sieved between 300 and 500 μm. The spacers and milled powders were then mixed in an appropriate volume ratio, loaded into a cylindrical steel mold, and compressed at 100 MPa pressure. The samples were vacuum sintered at 800 °C for 30 min and 2 h. The samples of 30 min and 2 h were then collected for XRD investigation and the grain size and lattice distortion were calculated according to the XRD patterns and Williamson-Hall equation. Density and porosity quantities of the specimen were additionally measured by Archimedes method. Moreover, optical images were used to determine the shape, size, and distribution of the pores. Phase transition temperatures were characterized by using differential scanning calorimeter (Rigaku PTC-10A) at heating/cooling rate of 10 °C/min and temperature range of -50 °C to 150 °C. Compression test was performed by dynamic testing machine (Zwick/Roel HCT 400/25, Germany) with a strain rate of 0.3 Cm/min at room temperature.

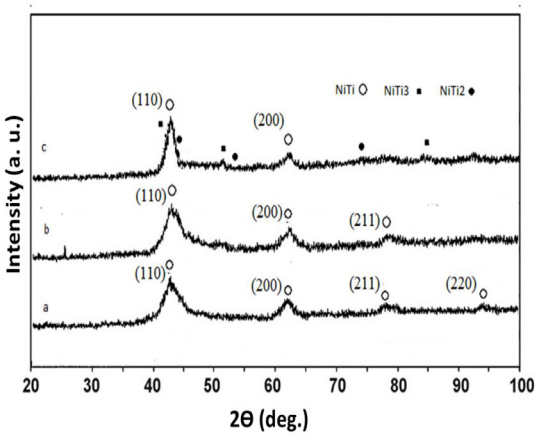

Fig. 1. XRD patterns of milled powder (a), sintered specimen at 800°C for 30 min (b), and the sintered specimen at 800°C for 120 min (c)

RESULTS AND DISCUSSION

XRD results

As reported by Gu et al., after 60 h of milling, the value of dissolved Ti in Ni would reach its maximum value which is 10.2 at.% [18]. Figure 1 shows the XRD patterns of the powder after 50 h milling and the sintered specimens. As it can be seen in Figure 1a, there is no elemental Ni or Ti characteristic peak, while broadened fundamental B2-NiTi peaks are present in the powder pattern. It is believed that the reason of disappearing of Ti and Ni peaks is the milling speed and time optimized for the procedure. It is worth noting that the presence of Ni and Ti elemental peaks after 30 h and 40 h of milling has been also reported in literature [17]. The equilibrium value of dissolved Ti in Ni was reported to be 6 at.% [19] at room temperature. However, by increasing the milling time and speed, there will be a high dislocation density and other structural defects which can lead to the formation of a supersaturated solid solution. The broadening of the NiTi peaks indicates the refinement of crystallite size or even formation of amorphous phase [17] that is the result of high dislocation density which provides easy diffusion's path for the atoms.

The adjustment of milling time and speed play an important role in the alloying process and the crystallite size. Ni and Ti powders are row materials. At the early stages of mechanical alloying, we will have NiTi and also Ti and Ni in the samples. However, by modifying milling time and speed, the mechanical alloying process will be continued and after 50 h of milling, there will be no elemental Ni or Ti peak in the XRD pattern. By increasing milling time, lattice parameter of Ni increases which lead to the formation of super saturated solid solution. On the other hand, increasing milling speed and time will cause reaching to nanoscale or amorphous phase. Ball mill is a common method for nanoparticles production. That is because of a high amount of work hardening in the process which result in high dislocation density and large amount of other structural defects.

In Figure 1b, the XRD pattern of the sintered specimens is presented. As the nanograin size and especially amorphous phase are unstable, sintering temperature and time should be optimized to avoid undesirable grain growth. It can be observed that the XRD pattern obtained for the sintered specimen is less broadened than the one of powder due to grain growth and crystallization of amorphous phase. Moreover, vacuumed furnace was employed to prevent oxidation and participation of undesired intermetallic phase. There is no peak of intermetallic phase in the XRD pattern.

The crystallite size can be derived by Williamson-Hall equation [20]:

$$B\cos\theta = 0.9\,\lambda/D + \varepsilon \sin\theta \quad (1)$$

Where B is the full-width at half maximum intensity, λ is the wavelength of the used XRD, D represents the average crystallite size, θ is the Bragg angle, and ε is the average strain.

Therefore, the grain size of powder and the sintered specimen were calculated to be 50 nm and 90 nm, respectively. The observed grain growth seems logical due to increased temperature employed in the procedure.

The XRD pattern of the specimen with 2h sintering time is presented in Figure 1c. Formation of some undesirable intermetallic compound can be seen. Increasing the sintering time leads to the formation of such compounds. The heat treatment can cause a deviation in the equality percentage of Ni and Ti which results in the formation of NiTi3 and $NiTi_2$.

Porosity

The powder was then mixed with the sieved spacers and pressed in the metallic mold. The samples were vacuumed sintered and the density of the specimens was determined after sintering using Archimedes method as following equation:

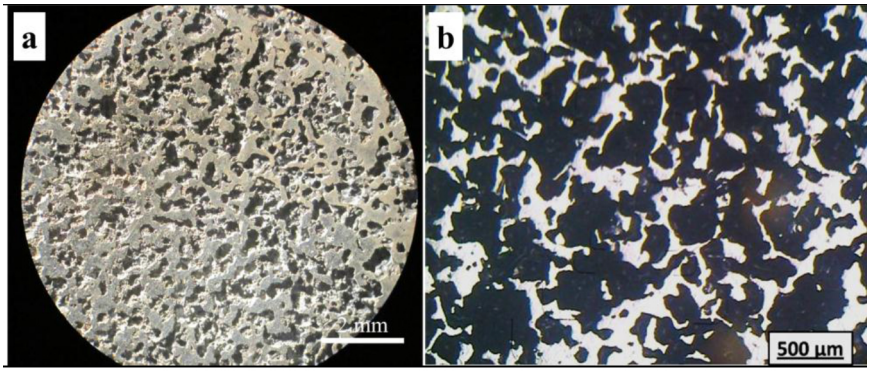

Fig. 2. Macroscopic image (a) and microscopic image (b) of the specimen with 70% porosity

$$\varepsilon_t = 100(1-\rho_b/\rho_t) \quad (2)$$

$$\rho_b = W_d/(w_e - W_a)\times\rho H_2O \quad (3)$$

Where εt is the true porosity percentage, ρt is the true density of the specimen, and ρb is the bulk density of the NiTi defined by Eq.3. W_d is the weight of the dry specimen, we are the weight of the specimen soaked with the immersion water and suspended in the air, and ρH_2O is the density of the pure water at the room temperature.

The porosity of the specimen was evaluated to be 70%. Besides, the amount of porosity, the pore size and distribution also plays an important role. The optical micrograph of the porous specimen is shown in Figure 2. It can be observed in Figure 2b that the obtained pore sizes are 300µm to 500µm due to sieved spacer diameter. It should be noted that such pore size is designated for orthopedic applications [7]. In Figure 2a homogeneous pore distribution can be seen in the macroscopic image of the specimen.

Transition temperatures

The DSC result of milled powder and the sintered sample are shown in Figure 3. As the pattern illustrates, there is just one transition in cooling and another one in the heating cycle for each specimen. The pattern presents B2↔R peaks and no R↔B19′ peaks are observed. In a study by Waitz et al., the results showed that B2↔B19′ transformation was effectively impeded when grain size was less than 100nm [21]. When the grain size decreases, there will be an increase in grain boundaries surface which leads to an increase in transformation energy barrier. Consequently, the self- accommodation twinning of B19′ martensite is delayed but B2↔R transition is not suppressed. In order to activate of B2↔R transition, the third element, precipitation or dislocation is essential. As it is mentioned above, high dislocation density in nano sample is the reason for occurring the B2↔R transition. However, the second specimen sintered for 2h showed no B2↔R transition while B2↔ B19′ can be seen in the pattern. Furthermore, this specimen does not have any of three situations which lead to R phase transition which indicates that the grain size of this specimen is too large to impede B2↔B19′ transition and shows typical NiTi transition. The obtained results have shown great agreement with data reported by Shi et al. [22] where decreasing nanograin size resulted in the increase of B2↔R transition temperature, but the decrease of R↔B19′ transition temperature.

Pressure test

Porous Nitinol shows a wide variety of mechanical features that can be explained due to porosity volume, shape, and distribution. It is possible to adjust some mechanical properties, such as elastic modules, pressure strength, etc. by controlling the porosity. A comparison of the stress-strain curves of the samples with two different sintering times is indicated in Fig.4. As it can be seen in Figure 4a the first specimen with 0.5 h sintering time shows a 5% recoverable strain. However, the second specimen which is sintered for 2h shows 3% recoverable strain (Figure 4b).

There is also a fracture in 2% strain for the sample with 2h sintering time. Mechanical properties of nanostructured materials have been widely investigated and the obtained data have shown that

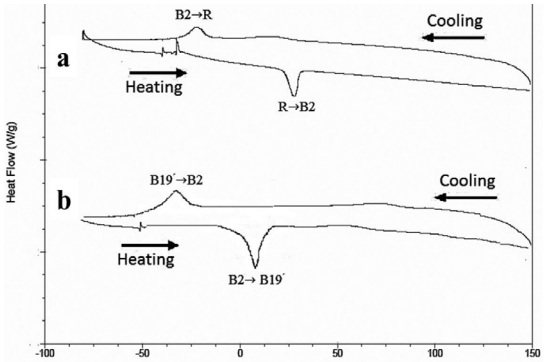

Fig. 3. DSC patterns of the sintered specimen at 800°C for 30 min (a), and the sintered specimen at 800°C for 120 min (b).

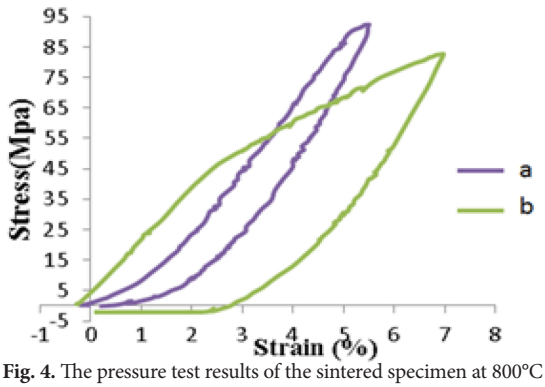

Fig. 4. The pressure test results of the sintered specimen at 800°C for 30 min (a), and the sintered specimen at 800°C for 120 min (b)

hardness and strength of nanostructure materials do not follow a clear manner and demonstrates much deviation from Hall–Petch equation [23]. But those discussions can be established for bulk nanostructured materials. The mechanical properties of porous nanostructure material are entirely similar to coarse grain structure and depend on porosity volume, morphology, and distribution. Hence, the difference between our two specimens can be explained by other factors such as porosity situation or intermetallic compounds rather than grain size.

The XRD pattern of the specimen with 2h sintering time shows some intermetallic compound including Ni3Ti and Ti2Ni. These compounds are brittle and usually pile up in grain boundaries. Therefore, it cannot be surprising that these intermetallic compounds are responsible for the mechanical properties of examined samples. Moreover, there is also a variance in elastic modules of loading cycle and unloading one due to the difference between elastic modules of Austenite phase (in loading cycle) and martensite phase (unloading cycle). Furthermore, a decrease in elastic modules is recorded as the result of porosity condition which can resolve the misfit problems raised due to the dissimilarity between elastic modules of NiTi and hard tissues.

CONCLUSIONS

In this study synthesis of porous nanostructured NiTi which is known as the most important material for manufacturing implants and other medical devises duo to its shape memory and superelasticity properties is investigated. It is shown that Nitinol can be synthesized in nanoscale grain size by milling at appropriate speed and time and also choosing proper sintering temperature and time. Nanostructure shows R phase transition. In fact, one of the effects of reaching to nanostructure is occurring R transformation due to high dislocation density and high grain boundaries surface. Nanostructured sample with 70% porosity was shown 5% superelasticity in the cyclic pressure test. Moreover, mechanical properties of porous nanostructure depend on porosity volume, shape and distribution rather than grain size. Moreover, one of the advantages of porous samples is their elastic modulus which is more similar to the bone than other metallic implants.

CONFLICTS OF INTEREST

The authors declare that there are no conflicts of interest regarding the publication of this manuscript.

REFERENCES

1. Kaynak Y, Karaca H, Noebe R, Jawahir I. Analysis of tool-wear and cutting force components in dry, preheated, and cryogenic machining of NiTi shape memory alloys, Procedia CIRP. 2013;8:498-503.
2. Ren H, Anuraj B, Dupont PE. Varying ultrasound power level to distinguish surgical instruments and tissue. Medical & biological engineering & computing, 2018;56(3):453-67.
3. La Rosa G, Savio FL, Pedullà E, Rapisarda E. A new torquemeter to measure the influence of heat-treatment on torsional resistance of NiTi endodontic instruments. Engineering Failure Analysis, 2017;82:446-57.
4. Gurley A, Lambert TR, Beale D, Broughton R. Dual measurement self-sensing technique of NiTi actuators

for use in robust control. Smart Materials and Structures, 2017;26(10):105050.

5. Hartl DJ, Lagoudas DC. Aerospace applications of shape memory alloys. Proceedings of the Institution of Mechanical Engineers, Part G: Journal of Aerospace Engineering, 2007;221(4):535-52.
6. Alarcon E, Heller L, Chirani SA, Šittner P, Kopeček J, Saint-Sulpice L, et al. Fatigue performance of superelastic NiTi near stress-induced martensitic transformation. International Journal of Fatigue, 2017;95:76-89.
7. Ghasemi A, Hosseini S, Sadrnezhaad S. Pore control in SMA NiTi scaffolds via space holder usage. Materials Science and Engineering: C, 2012;32(5):1266-70.
8. Itin V, Gyunter V, Shabalovskaya S, Sachdeva R. Mechanical properties and shape memory of porous nitinol. Materials characterization, 1994;32(3):179-87.
9. Andani MT, Saedi S, Turabi AS, Karamooz M, Haberland C, Karaca HE, et al. Mechanical and shape memory properties of porous Ni 50.1 Ti 49.9 alloys manufactured by selective laser melting. Journal of the Mechanical Behavior of Biomedical Materials, 2017;68:224-31.
10. Xia M, Liu P, Sun Q. Grain size dependence of Young's modulus and hardness for nanocrystalline NiTi shape memory alloy. Materials Letters, 2018;211:352-5.
11. Zhu S, Yang X, Fu D, Zhang L, Li C, Cui Z. Stress–strain behavior of porous NiTi alloys prepared by powders sintering. Materials Science and Engineering: A, 2005;408(1):264-8.
12. Farvizi M, Akbarpour MR, Yoon EY, Kim HS. Effect of high-pressure torsion on the microstructure and wear behavior of NiTi alloy. Metals and Materials International, 2015;21(5):891-6.
13. Guoxin H, Lixiang Z, Yunliang F, Yanhong L. Fabrication of high porous NiTi shape memory alloy by metal injection molding. Journal of materials processing technology, 2008;206(1):395-9.
14. Zhang L, Zhang Y, Jiang Y, Zhou R. Superelastic behaviors of biomedical porous NiTi alloy with high porosity and large pore size prepared by spark plasma sintering. Journal of Alloys and Compounds, 2015;644:513-22.
15. Kaya M, Orhan N, Tosun G. The effect of the combustion channels on the compressive strength of porous NiTi shape memory alloy fabricated by SHS as implant material. Current opinion in solid state and materials science, 2010;14(1):21-5.
16. Tian B, Tong Y, Chen F, Liu Y, Zheng Y. Phase transformation of NiTi shape memory alloy powders prepared by ball milling. Journal of Alloys and Compounds, 2009;477(1):576-9.
17. Mousavi T, Karimzadeh F, Abbasi M. Synthesis and characterization of nanocrystalline NiTi intermetallic by mechanical alloying. Materials Science and Engineering: A, 2008;487(1):46-51.
18. Suryanarayana C. Mechanical alloying and milling. Progress in materials science, 2001;46(1):1-184.
19. Gu Y, Goh C, Goi L, Lim C, Jarfors A, Tay B, et al. Solid state synthesis of nanocrystalline and/or amorphous 50Ni–50Ti alloy. Materials Science and Engineering: A, 2005;392(1):222-8.
20. Suryanarayana C, Grant N. A Practical Approach Plenum Press. New York. 1998.
21. Waitz T, Karnthaler H. Martensitic transformation of NiTi nanocrystals embedded in an amorphous matrix. Acta Materialia, 2004;52(19):5461-9.
22. Shi X, Guo F, Zhang J, Ding H, Cui L. Grain size effect on stress hysteresis of nanocrystalline NiTi alloys. Journal of Alloys and Compounds, 2016;688:62-8.
23. Zehetbauer MJ, Zhu YT. Bulk nanostructured materials: John Wiley & Sons; 2009.